

Imaging Challenges in Secondary Mitral Regurgitation Unsolved Issues and Perspectives

Patrizio Lancellotti, MD, PhD; Jose-Luis Zamorano, MD, PhD; Mani A. Vannan, MBBS

Chronic secondary mitral regurgitation (SMR) is a complex entity that is often clinically underappreciated.¹ It complicates either ischemic heart disease or dilated cardiomyopathy; its prevalence varies among series but may reach $\leq 50\%$ in patients with heart failure.² When present, SMR may exhibit a broad range of severity and confers an adverse prognosis, which is worse with increasing severity of mitral regurgitation (MR).^{3,4} The management of SMR poses a unique set of challenges, based partly on the complexity of the valve disorder and the still-evolving adoption of the optimal therapeutic approach.⁵ Noninvasive imaging and, in particular, echocardiography, plays a critical role for the initial and longitudinal assessment, for individual risk stratification and outcome prediction, and for guiding intervention in patients with chronic SMR.⁶

Cause, Mechanisms, and Structural Remodeling

SMR develops because of a combination of mitral leaflet tethering secondary to left ventricular (LV) dilatation/deformation with papillary displacement/discoordination, annular dilatation/dysfunction, insufficient LV-generated closing forces attributable to reduction of LV contractility, and global LV/papillary muscle dyssynchrony.^{1,5} Tethering of the mitral leaflets is the principal lesion of SMR and results in restriction of systolic leaflet motion, namely type IIIb of Carpentier's classification. SMR does not typically occur in global LV dysfunction without tethering. However, once tethering occurs, leaflet closure is further impaired by LV dysfunction because there is decreased force opposing tethering.⁶⁻⁹

The key event in the pathogenesis of SMR is the distortion of normal LV geometry—regional and global LV remodeling—with subsequent apical and lateral displacement of papillary muscles, which, in turn, draws the chordae tendineae away from the line of coaptation.^{7,8} The extent of LV systolic dysfunction and dilatation is weakly correlated to the degree of SMR unless accompanied by geometric distortion in the region of the papillary muscles.^{1,9} With progressive global/regional LV remodeling, the geometric distortion in the region of papillary muscles insertion increases and the SMR is worsened. However, in ischemic cardiomyopathy, SMR may be mitigated by papillary muscle elongation/remodeling via a reduction in leaflet tethering forces.¹⁰ Regional mechanical LV

dyssynchrony especially that involves the papillary muscles can promote SMR through a reduction in the systolic contraction of the posterior mitral annulus.¹¹ Global LV dyssynchrony contributes to SMR through a blunted LV systolic pressure rise resulting in decreased closing forces and leaving the leaflet deforming tethering forces relatively unopposed.^{12,13}

The morphological hallmark in SMR is the deformation of the mitral valve⁷ the extent of which is the major determinant of the degree of SMR.^{14,15} The retracted chordae tendineae secondary to LV remodeling and displacement of papillary muscles tether the valve leaflets, preventing normal valve closure and resulting in valvular incompetence. The tethering shape varies according to the site and extent of LV remodeling.¹⁶ In asymmetrical tethering, the tenting typically predominates in the region of the posterior-medial scallop of the posterior leaflet (P3) because of apically and posteriorly displaced posterior papillary muscle secondary to localized LV remodeling¹² (Figure 1). Tethering of secondary chords contributes to development of a hockey-stick deformity of the anterior leaflet.⁷ As a result, the coaptation point of the leaflets is displaced posteriorly with respect to the center of the LV cavity. The consequence is anterior leaflet over-ride with a posterior SMR jet. In symmetrical tethering, the coaptation point of the mitral valve is moved apically, with a large tenting and both leaflets are involved to a similar degree, causing a central regurgitant jet. Tethering is thus higher in patients with global LV remodeling^{16,17} (Figure 2). Alterations in mitral annulus size and shape contribute to the development of SMR as an adjunctive mechanism¹⁸ (Figure 3). In fact, patients with isolated mitral annular dilation in the absence of ventricular abnormalities show less MR than those with dilated cardiomyopathy, even after correction for annulus size.¹⁹ The normal mitral leaflet area is more than double the area of the annulus, indicating a significant reserve before annular enlargement can lead to noncoaptation. Annular dilatation is not limited to anterior-posterior region but extends to intertrigonal zone and results in loss of the typical saddle shape of the annulus, which reduces leaflet curvature and thereby increases leaflet stress.¹⁶ Alterations in annular contraction also interfere with leaflet coaptation and contribute to SMR. Severe asymmetrical LV remodeling in the basal inferoposterior LV and the consequent asymmetrical annular dilatation particularly exacerbate SMR because of less reduction in annular size during systole.⁵

Received January 27, 2014; accepted April 23, 2014.

From the Department of Cardiology, University of Liège Hospital, GIGA Cardiovascular Sciences, Heart Valve Clinic, University Hospital Sart Tilman, Liège, Belgium (P.L.); University Hospital Ramón y Cajal, Madrid, Spain (J.-L.Z.); and Piedmont Heart Institute, Atlanta, GA (M.A.V.).

Correspondence to Patrizio Lancellotti, MD, PhD, University of Liège, CHU Sart Tilman, Liège 4000, Belgium. E-mail plancellotti@chu.ulg.ac.be (*Circ Cardiovasc Imaging*. 2014;7:735-746.)

© 2014 American Heart Association, Inc.

Circ Cardiovasc Imaging is available at <http://circimaging.ahajournals.org>

DOI: 10.1161/CIRCIMAGING.114.000992

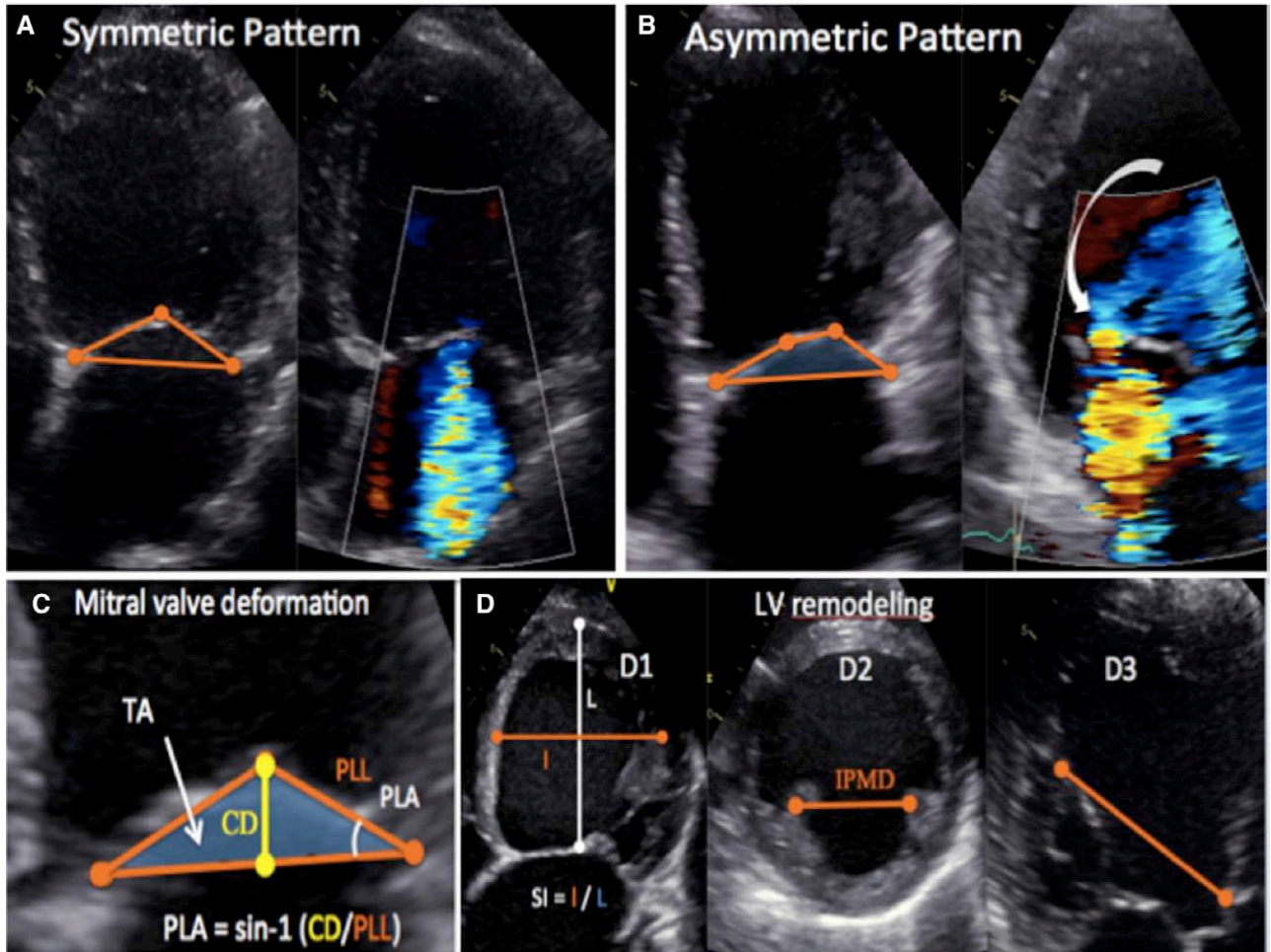


Figure 1. Assessment of mitral valvular deformation and global and regional left ventricular remodeling in patients with secondary mitral regurgitation. **A**, Symmetrical tenting pattern. **B**, Asymmetrical tenting pattern. **C**, Measurements of the tenting area (TA), coaptation distance (CD), and posterolateral angle (PLA). **D**, Measurements of the sphericity index (D1), interpapillary muscle distance (IPMD; D2), and apical displacement of the posteromedial papillary muscle (D3). PLL indicates posterior leaflet length; and SI, sphericity index.

In addition, mitral valve leaflets undergo progressive remodeling with elongation, stiffening, increase in matrix thickness, and fibrosis in response to the stresses imposed by increased leaflet tethering and mitral annular dilatation.^{20–22} The extent of this remodeling differs in individual

patients and for a similar degree of mitral leaflet tethering and LV remodeling, suggesting that leaflet enlargement is not attributable to a straightforward passive adaptation to leaflet stretch. In SMR, mitral leaflet area may increase by $\leq 35\%$ on average.²¹ However, such an adaptation is

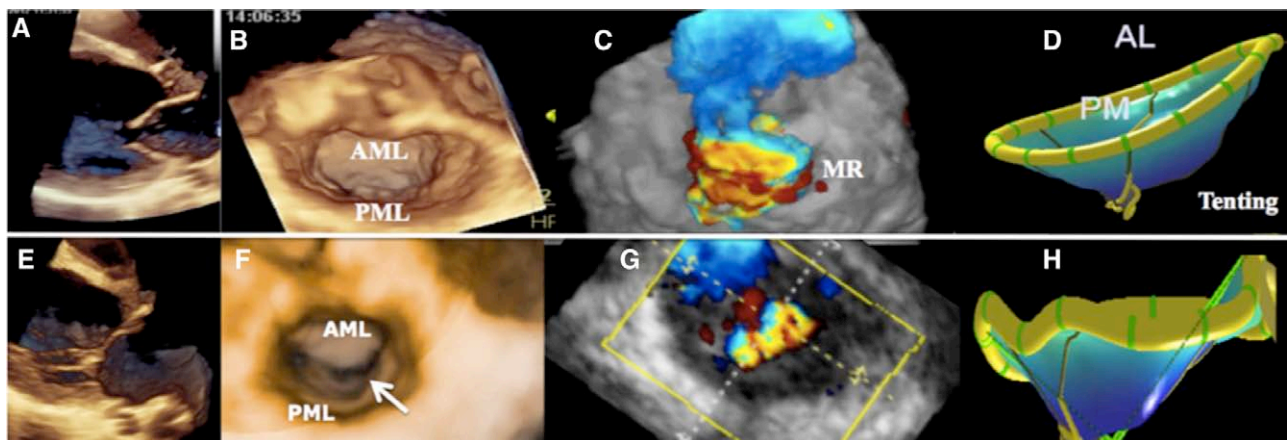


Figure 2. Patients with secondary mitral regurgitation. **A** to **D**, Symmetrical tenting pattern. **E** to **H**, Asymmetrical tenting pattern. **A** and **E**, Two-dimensional parasternal long-axis view. **B** and **F**, Three-dimensional volume rendering of the mitral valve. AML indicates anterior mitral leaflet; and PML, posterior mitral leaflet. **C** and **G**, Color flow of the regurgitant jet. **D** and **H**, Three-dimensional reconstruction of the tenting region. Arrow indicates zone of regurgitation.

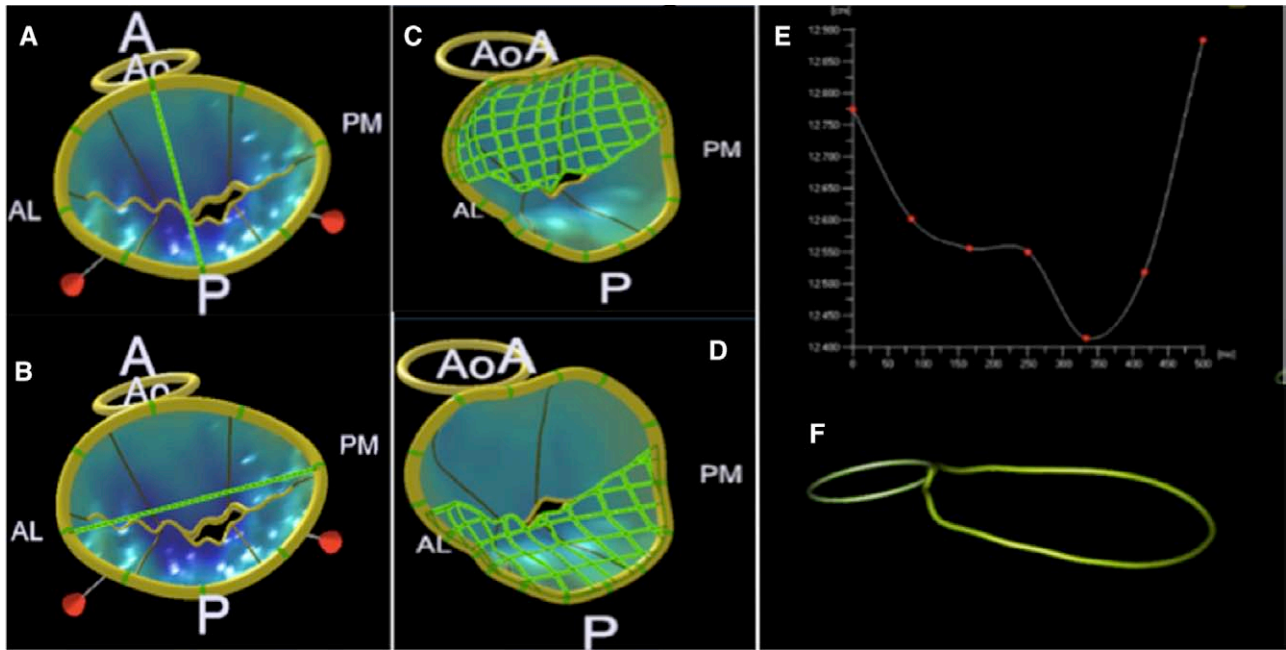


Figure 3. Three-dimensional (3D) reconstruction of the mitral annulus in secondary mitral regurgitation with measurements of the antero-posterior (A) and intercommissural (B) diameters, anterior (C) and posterior (D) leaflet surfaces, and dynamics of the mitral annulus (E). E, Dynamic motion analysis of the mitral annulus during the cardiac cycle. F, Schematic 3D representation of the mitral annulus, which appears flat, deformed, and no longer saddle shaped. A indicates anterior; AL, antero-lateral commissure; AO, aorta; P, posterior; and PM, papillary muscle.

often insufficient to meet the need for increased leaflet area imposed by the change in mitral valve configuration. Therefore, the discrepancy in leaflet area in relation to the required closure area (leaflet area/closure area) is an important determinant of the degree of MR.²² Interestingly, although valve enlargement can promote mitral coaptation, it can be a counterproductive by inducing maladaptive valve thickening, stiffness, and fibrosis.

Role of Imaging

Two-dimensional (2D) transthoracic and transesophageal echocardiography (TEE) play a substantial role in the evaluation of SMR.³ However, 3D echocardiography (3DE) has contributed most to the understanding of the structural remodeling that accompanies SMR.^{16–18} Three-dimensional echocardiography has demonstrated superiority over 2DE in measuring LV volumes, localizing and assessing the extent of mitral valve deformation, and determining the shape of the regurgitant orifice.¹¹ In patients with inadequate images or discrepant findings by echocardiography, cardiac magnetic resonance (CMR) can be used to quantify MR severity, evaluate LV anatomy and function, and assess the presence and extent of myocardial scar (late enhancement).²³ Cardiac computed tomography is rarely indicated in the evaluation of SMR, even if the extent of mitral valve deformation and MR severity might be assessed.²⁴ Cardiac computed tomography could be however useful in some cases to evaluate the coronary anatomy (ie, limited vascular access; Figure 4). Irrespective of imaging technique, the assessment of SMR needs to address findings related to mitral valve configuration, the severity of SMR, and LV remodeling because these features govern the indications for intervention and clinical outcomes.^{5,7}

Evaluation of Mitral Valve Configuration

The evaluation of mitral valve configuration should also include consideration of the MR jet direction.^{3,5} A posterior-directed jet (P2–P3) is usually associated with eccentric valve involvement and point of coaptation (asymmetrical tethering), whereas a central jet marks symmetrical involvement and point of coaptation (symmetrical tethering). Despite no evidence of structural mitral valve disease, the displacement of the leaflets into the LV leads to several morphological changes that can quantify the global and regional tethering burden.⁵ Annular dimensions, tenting area (region enclosed between the annulus and the mitral valve leaflets body), anterior and posterior leaflet angles, tenting height (vertical distance between the mitral annulus and the leaflet coaptation point), bending distances, and coaptation length/surface (a measure of coaptation reserve) are the commonest parameters measured.¹¹ With 2D echo, tethering is best appreciated in apical 4-chamber view but can be obtained from the parasternal long-axis view.⁹ With CMR, mitral valve anatomy is best imaged by acquisition of standard short-axis, 2-, 3-, and 4-chamber long-axis views in combination with oblique long-axis cines orthogonal to the line of coaptation.²³ However, the assessment of the exact location of the maximum tenting zone with 2D echo or CMR may be imprecise. Measures of mitral valve configuration parameters are now readily available using 3DE, which reduces the risk of foreshortened views and off-axis planes. Three-dimensional tenting volume correlates better with effective regurgitant orifice area (EROA) in patients with SMR.¹² Three-dimensional echocardiography also represents the method of choice to provide accurate evaluation of leaflets remodeling and mitral annulus dimensions and dynamics.^{25,26} For instance, the leaflet area/closure area and leaflet area/

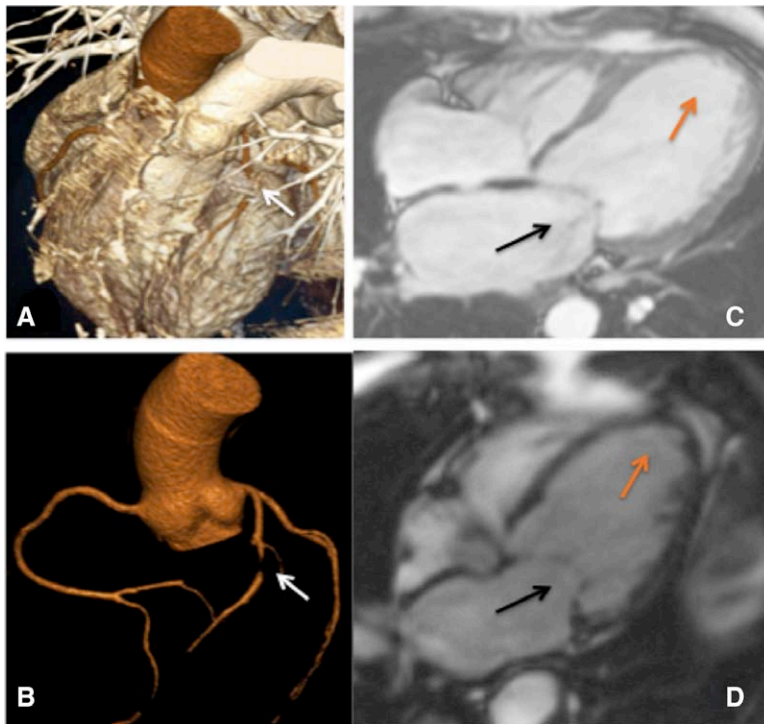


Figure 4. Patient with a history of anterior myocardial infarction, secondary mitral regurgitation, and severe left ventricular remodeling. Three-dimensional cardiac computed tomography showing a significant left anterior descending artery stenosis (**A** and **B**, white arrows). Cardiac magnetic resonance demonstrating the presence of significant mitral valve deformation, with a severe tenting (black arrows) and a large zone of myocardial scar (orange arrows; **C** and **D**).

annular area ratios and the 3D-derived indexes of coaptation are lower in patients with significant SMR.²⁴ However, it is not clear whether these 3D echo measurements provide incremental information to standard 2D echo measures for predicting outcome after treatment (Table 1).

Evaluation of LV Remodeling/Function

The location and extent of LV abnormalities/remodeling should be evaluated. The following findings are reported: LV volumes and shape (sphericity index), regional wall motion abnormalities, and markers of transmural necrosis (hyperechoic segments, diastolic thickness <5.5 mm, severe reduction in segmental strain, no contractile reserve, >50% late gadolinium enhancement [LGE]).²⁻⁶ LV ejection fraction and sphericity index (actual 3D volume compared with the volume of a sphere whose diameter is derived from the major LV long axis) are obtained preferably using 3D echo. When 3D is not available, the 2D biplane Simpson rule is recommended. With CMR, the LV dimensions are derived from a series of multisection perpendicular to the long axis of the LV (10–12 contiguous slices in short-axis direction). Regardless of the method used, because it is highly dependent on loading conditions, LV ejection fraction often overestimates the systolic function in case of significant SMR. Measurement of LV maximal dP/dt using continuous-wave Doppler of SMR jet can provide noninvasive estimation of global mitral closing forces.²¹ The parameters to be used to quantify LV dyssynchrony are controversial. Regional remodeling is quantified by the posterior and lateral displacements of 1 or both papillary muscles. Two-dimensional echo and CMR measurements include interpapillary muscle distance and posterior papillary–fibrosa distance. With 3D echo, the extent of papillary muscles displacement can be better evaluated. A specific advantage of CMR lies on the possibility to assess the presence and extent of myocardial

fibrosis, which can be either diffuse (quantification of myocardial extracellular expansion based on T1-mapping sequence) or focal (LGE). The more extensive the scar burden/focal fibrosis (LGE-CMR), the lower the likelihood of LV reverse remodeling after revascularization²⁷ or cardiac resynchronization therapy.²⁸ Cardiac computed tomography vein assessment in combination with LGE-CMR might be considered as reasonable options among other imaging tests (ie, invasive venous angiography, stress echocardiography, nuclear imaging) in patients thought to have extensive necrosis (Figure 5). The added value of T1-mapping to conventional LGE-CMR evaluation in patients with SMR still needs to be evaluated.

Assessment of Severity of MR

Echocardiographic assessment of the severity of SMR relies on an integrated approach using qualitative, semiquantitative, and quantitative parameters. A challenge in the evaluation of the degree of SMR is the temporal variation both within systole of a single cardiac cycle and during interval follow-up imaging related to loading conditions and changes in LV size.

Current Methods and Limitations

A combination of 2DE, spectral, and color Doppler parameters form the standard approach to quantify the degree of SMR.^{3,29} Despite the influence of settings, hemodynamic conditions, and mechanism of MR, the presence of a central color jet with a jet area <4 cm² or a jet that measures <10% (MR jet/left atrial area) is highly suggestive of mild SMR. On the contrary, large central MR jets reaching left atrial roof and pulmonary veins (with or without systolic spectral Doppler flow reversal) suggest significant MR. The vena contracta (VC) width in the parasternal long-axis view is another measure of the severity with a cutoff of ≥ 0.4 cm indicative of severe SMR.³⁰ It should be noted that although VC is relatively independent

Table 1. Two- and Three-Dimensional–Derived Echocardiographic Parameters Obtainable in SMR

Mitral Parameters	2D TEE	3D TEE
Annulus		
Intercommissural distance	+	++
Septolateral distance	+	++
Perimeter	+	++
Annulus height	–	++
Annulus dynamics	–	++
Leaflets		
Anterior leaflet area	–	++
Posterior leaflet area	–	++
Leaflet angle		
Posterior leaflet angle	+	++
Anterior leaflet angle	+	++
Coaptation		
Coaptation depth	+	++
Coaptation indexes	–	++
Leaflet coaptation area	–	++
Tethering		
Tenting area	+	+
Tenting volume	–	++
Ventricle		
LV end-diastolic volume	+	++
LV end-systolic volume	+	++
LV dyssynchrony (global/PMs)	+	++
Interpapillary distance		
PM tip	+	++
PM body	+	++
SMR evaluation		
PISA shape	+	++
Regurgitant orifice geometry	+	++

2D indicates 2-dimensional; LV, left ventricular; PM, papillary muscle; PISA, proximal isovelocity surface area; SMR, secondary mitral regurgitation; and TEE, transesophageal echocardiography.

of the driving pressure and flow rate, it is influenced by the dynamic variations in orifice area, which occurs with SMR. Calculation of EROA using the surface area of the proximal flow convergence (PFCR) is another approach to quantify SMR. The PFCR is imaged in the apical 4-chamber or apical long-axis view with appropriate settings, and the radius of the largest flow convergence in either view is used to measure the EROA using the standard formula assuming a hemispheric flow convergence. A cutoff EROA of ≥ 0.20 cm² is recommended for grading SMR as severe.³ Dynamic changes in MR, the predominant noncircular regular orifice shape, and constrained PFCR in the setting of regional myocardial deformity and leaflet tethering can limit the use and accuracy of the PFCR-based EROA computation in SMR. Regurgitant volume and fraction (RV/regurgitant fraction) in SMR is a valuable index of severity, but it is not routinely done by 2D echo/Doppler because of the need for cumbersome manual measurements in which small errors result in significant inaccuracies. Furthermore, individual measurements are made in

disparate cardiac cycles, which introduce further errors. An RV of ≥ 30 mL signifies severe SMR (Figure 6).

Newer Methods and Approaches

Recent advances in real-time 3D B-mode and color-flow Doppler (CFD) echocardiography have been valuable in making this technology more practical for routine clinical use.³¹ Furthermore, CMR may prove to be a good alternative and complementary to echocardiography in selective instances. Three-dimensional B-mode TEE and CMR studies show that the anatomic regurgitant orifice tend to track along the leaflet coaptation plane and have an elliptical, irregular, or linear shape in vast majority of patients with SMR.³² Manual planimetry of the orifice area yields anatomic regurgitant orifice area, which is an important adjunct to flow-based measures of EROA. The anatomic regurgitant orifice area closely tracks the color Doppler–based VC area.³³ The latter can be now obtained from 3D color Doppler imaging by both transthoracic echocardiography and TEE. A VC area of ≥ 0.41 cm² seems to be indicative of severe MR although further validation of this cutoff is necessary given that the comparison standard in most has been conventional 2D estimates of severity of MR. Also, the cutoff value for what constitutes severe SMR may be lower than in degenerative MR.³⁴ Despite these limitations, VC area is probably more accurate than VC width by 2D in SMR.^{35,36} Imaging the PFCR with 3D CFD has emphasized the considerable limitations of 2D-based computation of EROA. Several studies have confirmed that 3D is superior to 2D in more accurately characterizing the shape and the surface area of the PFCR in SMR. A more recent advancement in which the 3D surface area of the PFCR can be automatically measured and integrated during the duration of systole allows computation of a peak 3D EROA and integrated 3D RV by real-time volume CFD imaging. The latter has been specifically shown to be accurate when compared with CMR RV in SMR, although further confirmation of this is required in larger numbers and in multiple centers.³⁷ The intrinsic limitations of angle dependency of velocity profiles of the PFCR in relation to transducer location still apply to 3D CFD imaging, but it is more accurate than 2D in characterizing the shape, and automation makes it attractive for routine clinical application.

Another approach using real-time 3D volume CFD imaging is to measure mitral and LV outflow tract stroke volume and compute RV. The individual stroke volume can be measured automatically by integrating the volume color Doppler data and the area of the mitral annulus and LV outflow tract simultaneously through the cardiac cycle. This automated approach has been shown to be both more accurate and reproducible than using the spectral Doppler velocity profiles and 2D areas.³⁸ Furthermore, when extended specially to SMR, the RV/regurgitant fraction (regurgitant fraction) computed by this automated 3D CFD imaging compares well to CMR.³⁷ This promising single-center experience will need additional validation in a larger population. The presence of high-velocity aliasing in the LV outflow tract can limit the accuracy and the application of this technique just as the presence of multivalve disease. However, it does provide a solution in the presence of multiple MR jets, when VC and PFCR methods are not valid or reliable or to evaluate the residual MR through a dual orifice after MitraClip intervention.

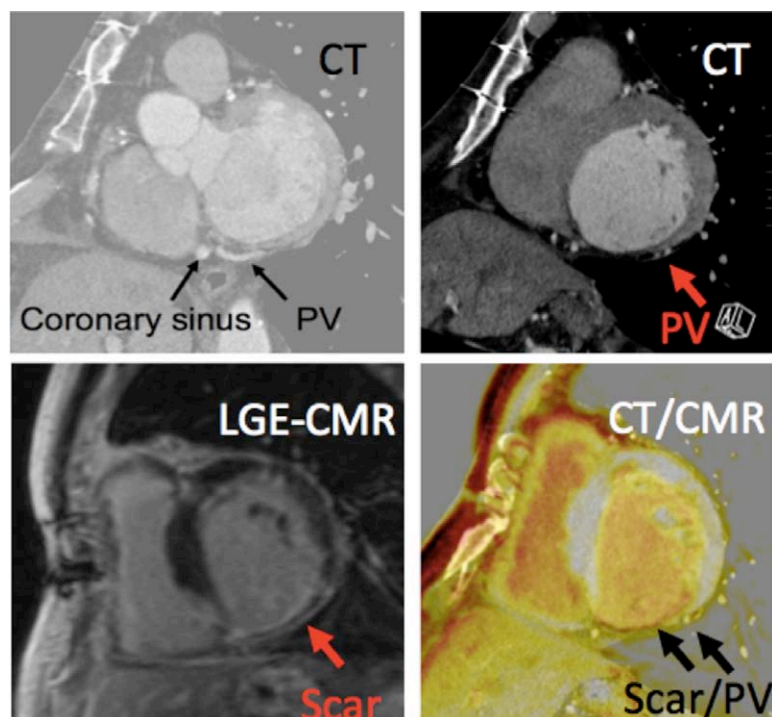


Figure 5. Cardiac computed tomography (CT) vein assessment in combination with late gadolinium enhancement (LGE-cardiac magnetic resonance [CMR]) in a patient with subendocardial infero-posterolateral myocardial infarction. PV indicates posterior vein.

CMR is a valuable adjunct to echocardiography in the evaluation of SMR (Figure 7).³⁹ When 2DE/3DE is available and optimal, the incremental role of CMR is limited with respect to grading severity of SMR. It is arguably superior to any echocardiographic approaches for the measurement of RV/regurgitant fraction. Similarly, accurate measurement of LV volume/size as an index of severity of MR may be potentially more accurate with CMR although 3DE is proving to be as good a technique and more practical. Although VC width, VC area, and anatomic regurgitant orifice area can be assessed by CMR,⁴⁰ it is only necessary when a combination of transthoracic echocardiography and TEE does not provide the information or there is discrepant information. The presence of atrial fibrillation in up to a third of patients with SMR further limits the use of CMR. The potential real strength of routine CMR in SMR may be in the assessment of the LV myocardial scar burden and perhaps mechanical function, which may predict clinical outcomes and success of interventions for SMR.

Imaging Interventions

Although interventions to treat SMR remain unsatisfactory with respect to survival benefit,^{41,42} there is evidence that reducing or abolishing SMR improves symptoms and attenuates progressive adverse LV remodeling.^{43,44} Interventional approaches have mainly focused on the mitral valve, and although various subvalvular techniques have been explored, there is no consensus on which of these are optimal. Recent advances in device-based therapies have further expanded the options in SMR, all of which have refocused the role of imaging in the selection, guidance, and postprocedural assessment.⁴⁵

Surgical Approaches

The predominant surgical technique is restrictive annuloplasty usually in the setting of coronary artery bypass grafting and in the presence of at least moderate SMR. The role of TEE

in restrictive annuloplasty is primarily to quantify the degree of MR and to quantify extent of mitral valve tethering. The presence of significant tethering does not preclude annuloplasty, but it seems to be predictive of residual and recurrent MR⁴⁶ (Table 2). Whether novel 3D parameters of mitral valve geometry (mitral leaflet size, annulus surface/area, coaptation indexes) by delineating the mechanisms associated with failure of annuloplasty improve the selection of patients and minimize procedural failure remains to be demonstrated. Similarly, whether the extent of preoperative LV remodeling is predictive of recurrent MR is still an ongoing question. Annuloplasty is performed with rings, which are specifically designed to accommodate the mitral annulus distortion (IMR ETlogix and GeoForm rings, Edwards Lifesciences, CA) without replicating the normal mitral annulus. Sizing the ring can be guided by intraoperative TEE. Figure 8 illustrates an example of how this can be done using intraoperative 3D TEE. The role of imaging in subvalvular approaches such as secondary chord cutting and repositioning of the papillary muscles is evolving, but preliminary reports of 3D modeling of papillary muscles and chords to aid interventions are encouraging and may help to reduce postoperative recurrence of MR.⁴⁷ When ventricular plication techniques are used, imaging may be a valuable aid to assess ventricular shape and size.

Device-Based Approaches

Cardiac resynchronization therapy⁹⁻¹⁴ and percutaneous mitral valve repair techniques⁴⁸ can decrease MR in selected groups of patients eligible for these treatments. Furthermore, there is also evidence for combined device approach or surgical–device approach to maximize the benefits of interventions in SMR.⁴⁹ Recent studies have applied stringent and varied inclusion criteria for device implantation and therefore have potentially excluded a substantial number of patients who might have benefited from these approaches and have included degenerative

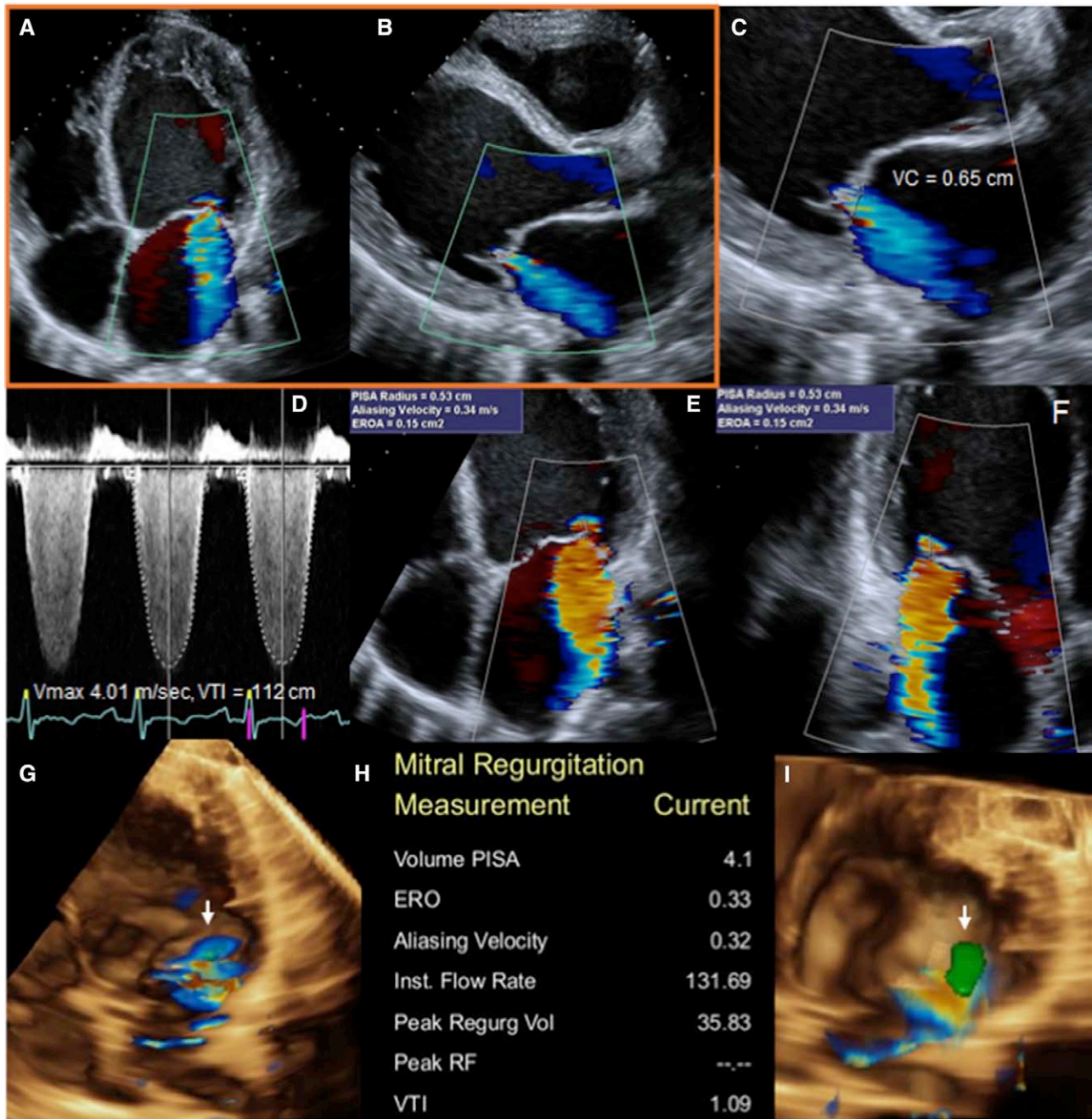


Figure 6. An illustrative example of secondary mitral regurgitation (SMR; **A** and **B**) in which 2-dimensional (2D) VCW (**C**) is consistent with moderate mitral regurgitation (MR). **D**, Measurement of the velocity time integral and peak velocity of the MR regurgitant jet using continuous wave Doppler. The 2D proximal flow convergence (PFCR)-based effective regurgitant orifice area (EROA) in the apical 4-chamber and apical long-axis views (**E** and **F**) is 0.15 cm² indicative of less than severe MR. Automated 3D surface area modeling by real-time 3D volume color-flow Doppler imaging (arrows in **G** and **I**) shows elliptical/noncircular orifice shape. Using the 3D surface area to compute the 3D PFCR-based EROA yields an orifice size of 0.33 cm² consistent with severe SMR. **H**, Data automatically calculated by the software. PISA indicates proximal isovelocity surface area; RF, regurgitant fraction; VCW, vena contracta width; and VTI, velocity time integral.

and SMR in 1 cohort applying the same cutoff for severity of MR.⁵⁰ Moreover, the disparate approach to defining imaging response to these device based may impede progress in this field. Thus, there is an urgent need to standardize selection of patients, guidance and assessment of procedural success, and definition of response versus nonresponse, especially with the ongoing Clinical Outcomes Assessment of the MitraClip Percutaneous Therapy for Extremely High-Surgical-Risk Patients (COAPT) and Randomized Study of the MitraClip Device In

Heart Failure Patients with Clinically Significant Functional Mitral Regurgitation (RESHAPE-HF) studies, which are focused on application of MitraClip to patients with SMR.

Unresolved Issues in Imaging Response to Treatment

Imaging can assess absence of MR after annuloplasty or replacement with accuracy, but evaluation of reduction of MR is more challenging especially when the postprocedural

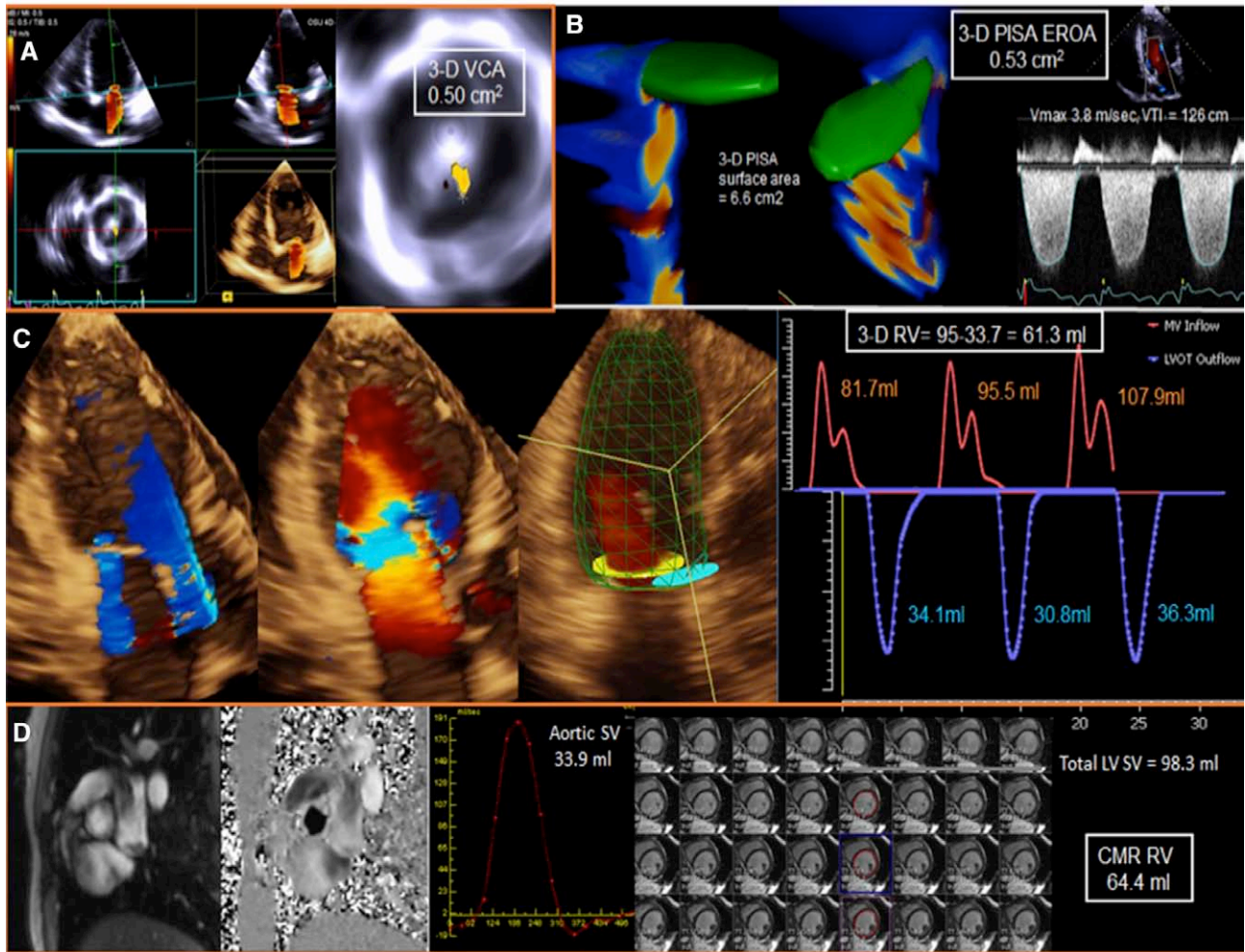


Figure 7. An illustrative example of secondary mitral regurgitation (SMR; **A** and **B**) in which 3-dimensional (3D) vena contracta area (VCA; **A**) by real-time volume color-flow Doppler (CFD) transthoracic echocardiography is 0.50 cm², consistent with severe mitral regurgitation (MR). The automated 3D proximal flow convergence (PFCR) modeling (**B**) shows a slit-like orifice shape, and using the 3D surface area yields an effective regurgitant orifice area (EROA) of 0.53 cm² consistent with the assessment by VCA of severe SMR. Automated mitral and aortic stroke volume (SV) measurement by real-time 3D volume CFD imaging (**C**, yellow and cyan blue disks track the mitral annulus and the left outflow tract [LVOT], respectively; the green mesh shows automated tracking of LV endocardial surface) yields a regurgitant volume (RV) of 61.2 mL. Measurement of aortic and total LV SV by cardiac magnetic resonance (CMR; **D**) shows an RV of 64.3 mL, comparable to RV by 3D CFD imaging. MV indicates mitral valve; PISA, proximal isovelocity surface area; and VTI, velocity time integral.

anatomy is unusual such as the double orifice after MitraClip implantation (Figure 9).⁴⁴ It is best to use the same integrative assessment to quantify residual MR as the one that is recommended for quantification of native SMR. The added value of 3D echocardiographic assessment of residual MR severity is unknown, but intuitively this would make sense, and data from ongoing prospective studies will help to ascertain this. At the present time, the definition of success of those procedures, which primarily reduce MR, remains unclear. The current imperfect practice in which an acceptable reduction in SMR is defined as a decrease by 1 grade in severity is perhaps the most practical. In the acute stage, an increase in forward stroke volume (>10%–15%) may also be a marker of good response to treatment. However, whether these responses necessarily translate into chronic improvement of cardiac performance is unknown. Similarly, a positive LV remodeling process after cardiac resynchronization therapy is defined as reduction in LV end-systolic volume (>10%–15%).⁵¹ However, the level to which the reduction in MR plays a role in

reverse LV remodeling remains unclear and requires to be evaluated prospectively. It may be also possible to better select patients and predict response in the future based on accumulated postprocedural imaging data on the degree of reduction in MR, positive LV remodeling, and clinical outcomes.⁵²

Imaging to Predict Progression and Clinical Outcomes

Disease progression in SMR is a complex interplay between LV remodeling which predates MR and the latter which can initiate and promote LV remodeling^{1–6} through increased wall stress and activation of neurohumoral mechanisms.^{20–22} SMR is fundamentally a ventricular disease; hence, the remodeling of the LV, the left atrium, and the mitral annulus are main determinants for predicting the progression of MR.⁵³ However, SMR begets progressive SMR as shown by Enriquez-Sarano et al⁵³ who reported an average yearly increase in RV of 1.5±9 mL and 0±5 mm² in EROA in a small group of patients (n=10). In addition, the presence of

Table 2. Preoperative Echocardiographic Parameters to Predict Annuloplasty Failure (Persistence and Recurrence of MR)

Parameter	TTE/TEE	Cutoff Value	Sensitivity/ Specificity, %
Mitral annulus diameter	TEE	≥37 mm	84/76
Tenting area	TTE	≥2.5 cm ²	64/95
Tenting area	TEE	≥1.6 cm ²	80/54
Coaptation distance	TTE	≥10 mm	64/90
Coaptation distance	TEE	≥10 mm	NA
Posterior leaflet angle	TTE	≥45°	100/95
Posterior leaflet tethering distance	TTE	≥40 mm	NA
Distal mitral anterior leaflet angle	TTE	>25°	88/94
Anterior mitral leaflet tethering angle	TTE	≥39.5°	NA
MR grade	TEE	≥3.5	42/81
MR jet	TTE	Central or complex	NA
LV end-systolic volume	TTE	≥145 mL	90/90
Systolic sphericity index	TTE	≥0.7	100/100
Wall motion score index	TTE	≥1.5	80/82
Interpapillary muscle distance	TTE	>20 mm	96/97

LV indicates left ventricular; MR, mitral regurgitation; NA, not available; TEE, transesophageal echocardiography; and TTE, transthoracic echocardiography.

dynamic changes in in the degree of SMR can accentuate the vicious cycle.⁵⁴

The presence and degree of SMR is associated with a 2-fold increase in mortality (38±5% versus 61±6%; $P<0.001$) after

myocardial infarction,⁵⁵ with increased mortality even in the presence of mild MR.⁵³ In patients with ischemic congestive heart failure and minimal or no symptoms⁵⁶ and in those with New York Heart Association II and III class,^{57–59} the presence of SMR, and especially in those with EROA ≥20 mm², mortality and morbidity was increased. Rossi et al⁴⁴ recently emphasized in a large multicenter study the importance of quantifying SMR to predict all-cause mortality or hospitalization for worsening of heart failure. Interestingly, their cohort included >400 patients with ischemic dilated cardiomyopathy. Even in idiopathic dilated cardiomyopathy,⁴⁴ severe SMR, defined as RV >30 mL or EROA ≥20 mm² or VC >0.4 cm, was associated with a 2-fold increased risk of adverse events after adjustment for LV ejection fraction and diastolic function. In a retrospective analysis of 2242 patients, the presence of moderate MR or even mild MR at the time of coronary artery bypass grafting was associated with lower 5-year postoperative survival as compared with patients without SMR (70±1%, 84±1%, and 86±1% for patients with moderate, mild, or no MR, respectively), even after adjustment for the degree of LV dysfunction and other comorbidities.⁵⁸ SMR is often dynamic with intermittent changes related to changes in loading conditions. An increase in EROA by ≥13 mm² during exercise is associated with reduced event-free survival, higher risk of heart failure, and major cardiac events compared with patients with no or mild increase or with decrease in MR severity.^{58–60}

Despite all this, debates still exist about whether SMR is only a marker of poor LV function or an independent risk factor for adverse outcome. Indeed, the severity of SMR tends to follow the severity of LV dysfunction causing SMR. Moreover,

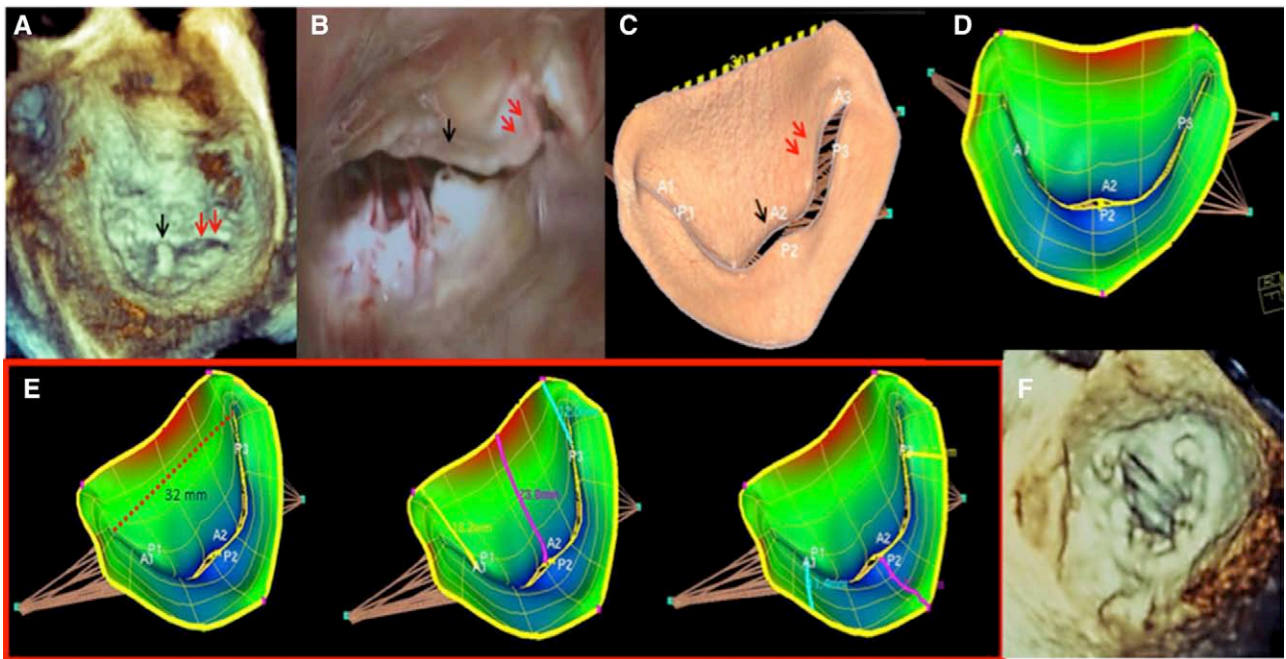


Figure 8. Three-dimensional (3D) transesophageal echocardiography (TEE) to guide mitral valve annuloplasty in secondary mitral regurgitation (SMR). Real-time 3D TEE shows the typical regurgitant orifice in SMR associated with posterior leaflet tethering (red arrows in **A**) and a single torn chord at P2 (black arrow in **A**) and the corresponding intraoperative findings (red and black arrows in **B**). Automated 3D TEE quantitative modeling also shows the regurgitant orifice (**C**) consequent to tethering (red arrows) and prolapse of P2 (black arrow). The extent of tethering is shown in blue hues in **D**. The 3D intercommissural distance can be automatically measured (red dotted line in **E**), the anterior leaflet height (pink line in **E**) can also be sized to guide selection of ring size, and the heights of the scallops of the posterior leaflet can also be sized (last figure in **E**). A Physio ring (30 mm, 1 size less than that predicted by the intercommissural distance/anterior leaflet height) was used for restrictive annuloplasty (**F**).

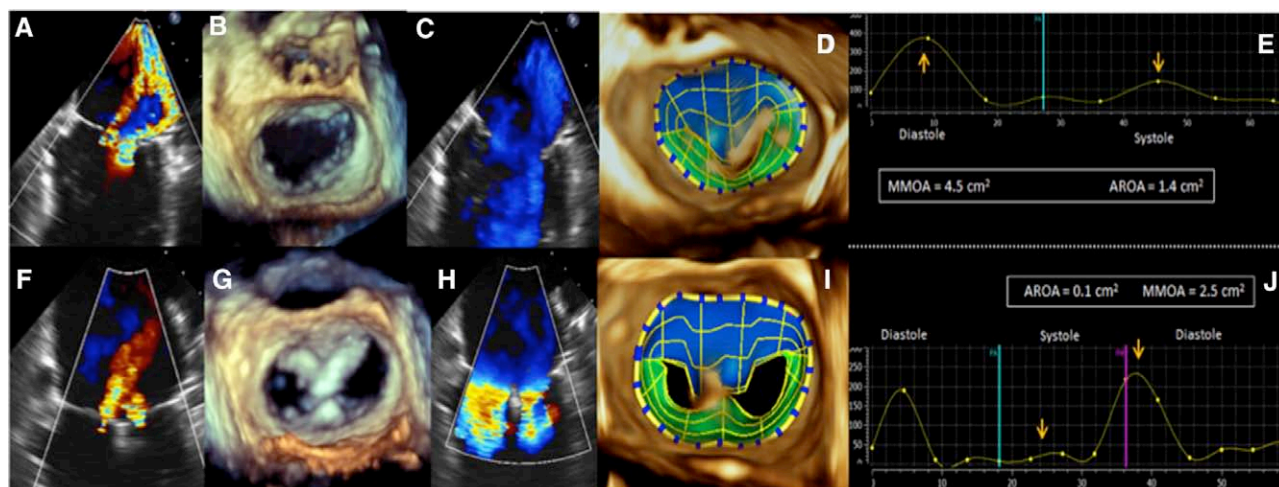


Figure 9. Three-dimensional (3D) transesophageal echocardiography (TEE) imaging of MitraClip for secondary mitral regurgitation (SMR). Two-dimensional color-flow Doppler (A) shows severe SMR, and 3D TEE shows single orifice in diastole (B). Color-flow Doppler in diastole (C) shows flow through the single orifice. Automated 3D modeling of the mitral valve shows a large anatomic regurgitant orifice (AROA) involving the A2/P2 and A3/P3 region (arrows in D) and the maximum 3D mitral orifice area (MMOA) and the AROA are 4.5 and 1.4 cm², respectively (E). Lower (F–I). Corresponding post-MitraClip images of double orifice and the dual jets of the MR are shown, and the postprocedure MMOA and AROA are 2.5 and 0.1 cm², respectively.

correcting SMR does not prolong life, which would be expected to occur if MR affected the outcome.^{41,42} Currently, no outcome studies using contemporary imaging techniques to quantify MR and evaluate LV function/remodeling have been conducted to address this dilemma. In this regard, large-scale studies examining the added value of 3DE and CMR are needed.

Future Directions

Better understanding of the origin and evolution of SMR is necessary to enable building more effective therapeutic strategies of this complex valvular disease. Detailed mapping of the geometric substrates promoting SMR will likely allow developing tailor-made innovative technical approaches targeted toward specific mechanisms. Advances in diagnostic imaging techniques will continue to play a major role in the assessment of SMR. Our role as imagers will be to identify the best imaging modalities in individual patients. The Progressions and Outcome of Secondary Mitral Regurgitation (POMAR) study has been specifically designed to address this question by comparing real-time 3D color transthoracic echocardiography and CMR imaging for the assessment of MR severity and LV remodeling.

Conclusions

A comprehensive evaluation of SMR includes the quantitative description of the structural changes in the LV and the mitral valve apparatus and the severity of MR predominantly using a combination of echocardiography and, if needed, of CMR. Whether newer techniques and technologies enhance the assessment of SMR and improve our ability to predict progression, outcomes, and guidance of therapy remains to be seen. Large multicenter studies that incorporate these newer approaches to image SMR may help to fill the current gaps in knowledge.

Disclosures

Dr Vannan receives research support from Siemens. The other authors report no conflicts.

References

- Levine RA, Schwammenthal E. Ischemic mitral regurgitation on the threshold of a solution: from paradoxes to unifying concepts. *Circulation*. 2005;112:745–758.
- Lancellotti P, Marwick T, Pierard LA. How to manage ischaemic mitral regurgitation. *Heart*. 2008;94:1497–1502.
- Lancellotti P, Tribouilloy C, Hagendorff A, Popescu BA, Edvardsen T, Pierard LA, Badano L, Zamorano JL; Scientific Document Committee of the European Association of Cardiovascular Imaging. Recommendations for the echocardiographic assessment of native valvular regurgitation: an executive summary from the European Association of Cardiovascular Imaging. *Eur Heart J Cardiovasc Imaging*. 2013;14:611–644.
- Piérard LA, Carabello BA. Ischaemic mitral regurgitation: pathophysiology, outcomes and the conundrum of treatment. *Eur Heart J*. 2010;31:2996–3005.
- Marwick TH, Lancellotti P, Pierard L. Ischaemic mitral regurgitation: mechanisms and diagnosis. *Heart*. 2009;95:1711–1718.
- Silbiger JJ. Novel pathogenetic mechanisms and structural adaptations in ischemic mitral regurgitation. *J Am Soc Echocardiogr*. 2013;26:1107–1117.
- Ciarka A, Van de Veire N. Secondary mitral regurgitation: pathophysiology, diagnosis, and treatment. *Heart*. 2011;97:1012–1023.
- He S, Fontaine AA, Schwammenthal E, Yoganathan AP, Levine RA. Integrated mechanism for functional mitral regurgitation: leaflet restriction versus coapting force: *in vitro* studies. *Circulation*. 1997;96:1826–1834.
- Otsuji Y, Handschumacher MD, Liel-Cohen N, Tanabe H, Jiang L, Schwammenthal E, Guerrero JL, Nicholls LA, Vlahakes GJ, Levine RA. Mechanism of ischemic mitral regurgitation with segmental left ventricular dysfunction: three-dimensional echocardiographic studies in models of acute and chronic progressive regurgitation. *J Am Coll Cardiol*. 2001;37:641–648.
- Lancellotti P, Mélon P, Sakalihan N, Waleffe A, Dubois C, Bertholet M, Piérard LA. Effect of cardiac resynchronization therapy on functional mitral regurgitation in heart failure. *Am J Cardiol*. 2004;94:1462–1465.
- Ypenburg C, Lancellotti P, Tops LF, Bleeker GB, Holman ER, Piérard LA, Schalij MJ, Bax JJ. Acute effects of initiation and withdrawal of cardiac resynchronization therapy on papillary muscle dyssynchrony and mitral regurgitation. *J Am Coll Cardiol*. 2007;50:2071–2077.
- Breithardt OA, Sinha AM, Schwammenthal E, Bidaoui N, Markus KU, Franke A, Stellbrink C. Acute effects of cardiac resynchronization therapy on functional mitral regurgitation in advanced systolic heart failure. *J Am Coll Cardiol*. 2003;41:765–770.
- Ypenburg C, Lancellotti P, Tops LF, Boersma E, Bleeker GB, Holman ER, Thomas JD, Schalij MJ, Piérard LA, Bax JJ. Mechanism of improvement in mitral regurgitation after cardiac resynchronization therapy. *Eur Heart J*. 2008;29:757–765.

14. Lancellotti P, Lebrun F, Piérard LA. Determinants of exercise-induced changes in mitral regurgitation in patients with coronary artery disease and left ventricular dysfunction. *J Am Coll Cardiol*. 2003;42:1921–1928.
15. Yiu SF, Enriquez-Sarano M, Tribouilloy C, Seward JB, Tajik AJ. Determinants of the degree of functional mitral regurgitation in patients with systolic left ventricular dysfunction: a quantitative clinical study. *Circulation*. 2000;102:1400–1406.
16. Fattouch K, Castrovinci S, Murana G, Novo G, Caccamo G, Bertolino EC, Sampognaro R, Novo S, Ruvolo G, Lancellotti P. Multiplane two-dimensional versus real time three-dimensional transesophageal echocardiography in ischemic mitral regurgitation. *Echocardiography*. 2011;28:1125–1132.
17. Watanabe N, Ogasawara Y, Yamaura Y, Kawamoto T, Toyota E, Akasaka T, Yoshida K. Quantitation of mitral valve tenting in ischemic mitral regurgitation by transthoracic real-time three-dimensional echocardiography. *J Am Coll Cardiol*. 2005;45:763–769.
18. Watanabe N, Ogasawara Y, Yamaura Y, Wada N, Kawamoto T, Toyota E, Akasaka T, Yoshida K. Mitral annulus flattens in ischemic mitral regurgitation: geometric differences between inferior and anterior myocardial infarction: a real-time 3-dimensional echocardiographic study. *Circulation*. 2005;112(9 suppl):1458–1462.
19. Otsuji Y, Kumanohoso T, Yoshifuku S, Matsukida K, Koriyama C, Kisanuki A, Minagoe S, Levine RA, Tei C. Isolated annular dilation does not usually cause important functional mitral regurgitation: comparison between patients with lone atrial fibrillation and those with idiopathic or ischemic cardiomyopathy. *J Am Coll Cardiol*. 2002;39:1651–1656.
20. Dal-Bianco JP, Aikawa E, Bischoff J, Guerrero JL, Handschumacher MD, Sullivan S, Johnson B, Titus JS, Iwamoto Y, Wylie-Sears J, Levine RA, Carpentier A. Active adaptation of the tethered mitral valve: insights into a compensatory mechanism for functional mitral regurgitation. *Circulation*. 2009;120:334–342.
21. Chaput M, Handschumacher MD, Tournoux F, Hua L, Guerrero JL, Vlahakes GJ, Levine RA. Mitral leaflet adaptation to ventricular remodeling: occurrence and adequacy in patients with functional mitral regurgitation. *Circulation*. 2008;118:845–852.
22. Saito K, Okura H, Watanabe N, Obase K, Tamada T, Koyama T, Hayashida A, Neishi Y, Kawamoto T, Yoshida K. Influence of chronic tethering of the mitral valve on mitral leaflet size and coaptation in functional mitral regurgitation. *JACC Cardiovasc Imaging*. 2012;5:337–345.
23. Christiansen JP, Karamitsos TD, Myerson SG. Assessment of valvular heart disease by cardiovascular magnetic resonance imaging: a review. *Heart Lung Circ*. 2011;20:73–82.
24. Beaudoin J, Thai WE, Wai B, Handschumacher MD, Levine RA, Truong QA. Assessment of mitral valve adaptation with gated cardiac computed tomography: validation with three-dimensional echocardiography and mechanistic insight to functional mitral regurgitation. *Circ Cardiovasc Imaging*. 2013;6:784–789.
25. Levack MM, Jassar AS, Shang EK, Vergnat M, Woo YJ, Acker MA, Jackson BM, Gorman JH 3rd, Gorman RC. Three-dimensional echocardiographic analysis of mitral annular dynamics: implication for annuloplasty selection. *Circulation*. 2012;126(11 suppl 1):S183–S188.
26. Vergnat M, Jassar AS, Jackson BM, Ryan LP, Eperjesi TJ, Pouch AM, Weiss SJ, Cheung AT, Acker MA, Gorman JH 3rd, Gorman RC. Ischemic mitral regurgitation: a quantitative three-dimensional echocardiographic analysis. *Ann Thorac Surg*. 2011;91:157–164.
27. Chan J, Khafagi F, Young AA, Cowan BR, Thompson C, Marwick TH. Impact of coronary revascularization and transmural extent of scar on regional left ventricular remodeling. *Eur Heart J*. 2008;29:1608–1617.
28. Bleeker GB, Kaandorp TA, Lamb HJ, Boersma E, Steendijk P, de Roos A, van der Wall EE, Schalij MJ, Bax JJ. Effect of posterolateral scar tissue on clinical and echocardiographic improvement after cardiac resynchronization therapy. *Circulation*. 2006;113:969–976.
29. Grayburn PA, Weissman NJ, Zamorano JL. Quantitation of mitral regurgitation. *Circulation*. 2012;126:2005–2017.
30. Heinle SK, Hall SA, Brickner ME, Willett DL, Grayburn PA. Comparison of vena contracta width by multiplane transesophageal echocardiography with quantitative Doppler assessment of mitral regurgitation. *Am J Cardiol*. 1998;81:175–179.
31. Zamorano JL, Gonçalves A. Three dimensional echocardiography for quantification of valvular heart disease. *Heart*. 2013;99:811–818.
32. Yosefy C, Levine RA, Solis J, Vaturi M, Handschumacher MD, Hung J. Proximal flow convergence region as assessed by real-time 3-dimensional echocardiography: challenging the hemispheric assumption. *J Am Soc Echocardiogr*. 2007;20:389–396.
33. de Agustin JA, Marcos-Alberca P, Fernandez-Golfin C, Zamorano J. Direct measurement of proximal isovelocity surface area by single-beat three-dimensional color Doppler echocardiography in mitral regurgitation: a validation study. *J Am Soc Echocardiogr*. 2012; 25: 815–23.
34. Thavendiranathan P, Phelan D, Thomas JD, Flamm SD, Marwick TH. Quantitative assessment of mitral regurgitation: validation of new methods. *J Am Coll Cardiol*. 2012;60:1470–1483.
35. Kahlert P, Plicht B, Schenk IM, Janosi RA, Erbel R, Buck T. Direct assessment of size and shape of noncircular vena contracta area in functional versus organic mitral regurgitation using real-time three-dimensional echocardiography. *J Am Soc Echocardiogr*. 2008;21:912–921.
36. Zeng X, Levine RA, Hua L, Morris EL, Kang Y, Flaherty M, Morgan NV, Hung J. Diagnostic value of vena contracta area in the quantification of mitral regurgitation severity by color Doppler 3D echocardiography. *Circ Cardiovasc Imaging*. 2011;4:506–513.
37. Thavendiranathan P, Liu S, Datta S, Rajagopalan S, Ryan T, Igo SR, Jackson MS, Little SH, De Michelis N, Vannan MA. Quantification of chronic functional mitral regurgitation by automated 3-dimensional peak and integrated proximal isovelocity surface area and stroke volume techniques using real-time 3-dimensional volume color Doppler echocardiography: *in vitro* and clinical validation. *Circ Cardiovasc Imaging*. 2013;6:125–133.
38. Thavendiranathan P, Liu S, Datta S, Walls M, Nitinunu A, Van Houten T, Tomson NA, Vidmar L, Georgescu B, Wang Y, Srinivasan S, De Michelis N, Raman SV, Ryan T, Vannan MA. Automated quantification of mitral inflow and aortic outflow stroke volumes by three-dimensional real-time volume color-flow Doppler transthoracic echocardiography: comparison with pulsed-wave Doppler and cardiac magnetic resonance imaging. *J Am Soc Echocardiogr*. 2012;25:56–65.
39. Thavendiranathan P, Phelan D, Collier P, Thomas JD, Flamm SD, Marwick TH. Quantitative assessment of mitral regurgitation: how best to do it. *JACC Cardiovasc Imaging*. 2012;5:1161–1175.
40. Thavendiranathan P, Phelan D, Thomas JD, Flamm SD, Marwick TH. Quantitative assessment of mitral regurgitation: validation of new methods. *J Am Coll Cardiol*. 2012;60:1470–1483.
41. Chan KM, Punjabi PP, Flather M, Wage R, Symmonds K, Roussin I, Rahman-Haley S, Pennell DJ, Kilner PJ, Dreyfus GD, Pepper JR; RIME Investigators. Coronary artery bypass surgery with or without mitral valve annuloplasty in moderate functional ischemic mitral regurgitation: final results of the Randomized Ischemic Mitral Evaluation (RIME) trial. *Circulation*. 2012;126:2502–2510.
42. Acker MA, Parides MK, Perrault LP, Moskowitz AJ, Gelijns AC, Voisine P, Smith PK, Hung JW, Blackstone EH, Puskas JD, Argenziano M, Gammie JS, Mack M, Ascheim DD, Bagiella E, Moquete EG, Ferguson TB, Horvath KA, Geller NL, Miller MA, Woo YJ, D'Alessandro DA, Ailawadi G, Dagenais F, Gardner TJ, O'Gara PT, Michler RE, Kron IL; CTSN. Mitral-valve repair versus replacement for severe ischemic mitral regurgitation. *N Engl J Med*. 2014;370:23–32.
43. Deja MA, Grayburn PA, Sun B, Rao V, She L, Krejca M, Jain AR, Leng Chua Y, Daly R, Senni M, Mokrzycki K, Menicanti L, Oh JK, Michler R, Wróbel K, Lamy A, Velazquez EJ, Lee KL, Jones RH. Influence of mitral regurgitation repair on survival in the surgical treatment for ischemic heart failure trial. *Circulation*. 2012;125:2639–2648.
44. Rossi A, Dini FL, Faggiano P, Agricola E, Cicoira M, Frattini S, Simioniu A, Gullace M, Ghio S, Enriquez-Sarano M, Temporelli PL. Independent prognostic value of functional mitral regurgitation in patients with heart failure. A quantitative analysis of 1256 patients with ischaemic and non-ischaemic dilated cardiomyopathy. *Heart*. 2011;97:1675–1680.
45. Zamorano JL, Badano LP, Bruce C, Chan KL, Gonçalves A, Hahn RT, Keane MG, La Canna G, Monaghan MJ, Nihoyannopoulos P, Silvestry FE, Vanoverschelde JL, Gillam LD. EAE/ASE recommendations for the use of echocardiography in new transcatheter interventions for valvular heart disease. *Eur Heart J*. 2011;32:2189–2214.
46. Zhu F, Otsuji Y, Yotsumoto G, Yuasa T, Ueno T, Yu B, Koriyama C, Hamasaki S, Biro S, Kisanuki A, Minagoe S, Levine RA, Sakata R, Tei C. Mechanism of persistent ischemic mitral regurgitation after annuloplasty: importance of augmented posterior mitral leaflet tethering. *Circulation*. 2005;112(9 suppl):I396–I401.
47. Fattouch K, Lancellotti P, Castrovinci S, Murana G, Sampognaro R, Corrado E, Caruso M, Speziale G, Novo S, Ruvolo G. Papillary muscle relocation in conjunction with valve annuloplasty improve repair results in severe ischemic mitral regurgitation. *J Thorac Cardiovasc Surg*. 2012;143:1352–1355.
48. Franzen O, van der Heyden J, Baldus S, Schlüter M, Schillinger W, Butter C, Hoffmann R, Corti R, Pedrazzini G, Swaans MJ, Neuss M, Rudolph V, Sürder D, Grünenfelder J, Eulenburg C, Reichenspurner H,

- Meinertz T, Auricchio A. MitraClip® therapy in patients with end-stage systolic heart failure. *Eur J Heart Fail*. 2011;13:569–576.
49. Auricchio A, Schillinger W, Meyer S, Maisano F, Hoffmann R, Ussia GP, Pedrazzini GB, van der Heyden J, Fratini S, Klersy C, Komtebedde J, Franzen O; PERMIT-CARE Investigators. Correction of mitral regurgitation in nonresponders to cardiac resynchronization therapy by MitraClip improves symptoms and promotes reverse remodeling. *J Am Coll Cardiol*. 2011;58:2183–2189.
 50. Mauri L, Foster E, Glower DD, Apruzzese P, Massaro JM, Herrmann HC, Hermiller J, Gray W, Wang A, Pedersen WR, Bajwa T, Lasala J, Low R, Grayburn P, Feldman T; EVEREST II Investigators. 4-year results of a randomized controlled trial of percutaneous repair versus surgery for mitral regurgitation. *J Am Coll Cardiol*. 2013;62:317–328.
 51. Sénéchal M, Lancellotti P, Magne J, Garceau P, Champagne J, Philippon F, O'Hara G, Moonen M, Dubois M. Impact of mitral regurgitation and myocardial viability on left ventricular reverse remodeling after cardiac resynchronization therapy in patients with ischemic cardiomyopathy. *Am J Cardiol*. 2010;106:31–37.
 52. Beaudoin J, Levine RA, Guerrero JL, Yosefy C, Sullivan S, Abedat S, Handschumacher MD, Szymanski C, Gilon D, Palmeri NO, Vlahakes GJ, Hajjar RJ, Beer R. Late repair of ischemic mitral regurgitation does not prevent left ventricular remodeling: importance of timing for beneficial repair. *Circulation*. 2013;128(11 suppl 1):S248–S252.
 53. Enriquez-Sarano M, Basmdjian AJ, Rossi A, Bailey KR, Seward JB, Tajik AJ. Progression of mitral regurgitation: a prospective Doppler echocardiographic study. *J Am Coll Cardiol*. 1999;34:1137–1144.
 54. Lancellotti P, Magne J. Stress echocardiography in regurgitant valve disease. *Circ Cardiovasc Imaging*. 2013;6:840–849.
 55. Grigioni F, Enriquez-Sarano M, Zehr KJ, Bailey KR, Tajik AJ. Ischemic mitral regurgitation: long-term outcome and prognostic implications with quantitative Doppler assessment. *Circulation*. 2001;103:1759–1764.
 56. Grigioni F, Detaint D, Avierinos JF, Scott C, Tajik J, Enriquez-Sarano M. Contribution of ischemic mitral regurgitation to congestive heart failure after myocardial infarction. *J Am Coll Cardiol*. 2005;45:260–267.
 57. Lancellotti P, Troisfontaines P, Toussaint AC, Pierard LA. Prognostic importance of exercise-induced changes in mitral regurgitation in patients with chronic ischemic left ventricular dysfunction. *Circulation*. 2003;108:1713–1717.
 58. Piérard LA, Lancellotti P. The role of ischemic mitral regurgitation in the pathogenesis of acute pulmonary edema. *N Engl J Med*. 2004;351:1627–1634.
 59. Lancellotti P, Gérard PL, Piérard LA. Long-term outcome of patients with heart failure and dynamic functional mitral regurgitation. *Eur Heart J*. 2005;26:1528–1532.
 60. Grossi EA, Crooke GA, DiGiorgi PL, Schwartz CF, Jorde U, Applebaum RM, Ribakove GH, Galloway AC, Grau JB, Colvin SB. Impact of moderate functional mitral insufficiency in patients undergoing surgical revascularization. *Circulation*. 2006;114(1 suppl):I573–I576.

KEY WORDS: echocardiography ■ heart failure ■ mitral valve insufficiency ■ prognosis

Imaging Challenges in Secondary Mitral Regurgitation: Unsolved Issues and Perspectives

Patrizio Lancellotti, Jose-Luis Zamorano and Mani A. Vannan

Circ Cardiovasc Imaging. 2014;7:735-746
doi: 10.1161/CIRCIMAGING.114.000992

Circulation: Cardiovascular Imaging is published by the American Heart Association, 7272 Greenville Avenue,
Dallas, TX 75231

Copyright © 2014 American Heart Association, Inc. All rights reserved.
Print ISSN: 1941-9651. Online ISSN: 1942-0080

The online version of this article, along with updated information and services, is located on the
World Wide Web at:

<http://circimaging.ahajournals.org/content/7/4/735>

Permissions: Requests for permissions to reproduce figures, tables, or portions of articles originally published in *Circulation: Cardiovascular Imaging* can be obtained via RightsLink, a service of the Copyright Clearance Center, not the Editorial Office. Once the online version of the published article for which permission is being requested is located, click Request Permissions in the middle column of the Web page under Services. Further information about this process is available in the [Permissions and Rights Question and Answer](#) document.

Reprints: Information about reprints can be found online at:
<http://www.lww.com/reprints>

Subscriptions: Information about subscribing to *Circulation: Cardiovascular Imaging* is online at:
<http://circimaging.ahajournals.org/subscriptions/>